Shape Separation of Gold Nanostars using Density Gradient Centrifugation

A thesis submitted towards partial fulfillment of the
BS-MS Dual Degree Programme
by

Vished
Indian Institute of Science Education & Research, Pune

Under the Guidance of

Professor Teri W. Odom
Associate Chair
Department of Chemistry
Northwestern University, USA

Certificate

This is to certify that this dissertation entitled "***Shape Separation of Gold NanoStars using Density Gradient Centrifugation***" towards the partial fulfillment of the BS-MS dual degree programme at the Indian Institute of Science Education and Research, Pune represents original research carried out by ***Vished*** at *Northwestern University* under the supervision of ***Professor Teri Wang Odom****, Associate Chair & Professor of Chemistry, Material Science and Engineering* at Department of Chemistry during the academic year 2016-2017.

_____ 03/29/2017

Prof. Teri W. Odom Date

Declaration

I hereby declare that the matter embodied in the report entitled "***Shape Separation of Gold NanoStars using Density Gradient Centrifugation"*** are the results of the investigations carried out by me at the Department of Chemistry, *Northwestern University*, under the supervision of ***Professor Teri W. Odom*** and the same has not been submitted elsewhere for any other degree.

_____ 03/29/2017

Vished
(20121041)

Date

Acknowledgement

The success of this project required a lot of guidance and assistance from many people, and I feel extremely fortunate to have got this all along the completion of my project. I would like to take this opportunity to express my gratitude and appreciation to all those who encouraged and helped me to complete this project.

First and foremost, I would like to make my deepest appreciation and gratitude to my mentor Prof. Teri W. Odom, who was extremely helpful and offered invaluable guidance during the project. I am very grateful to her for allowing me to be a part of the Odom Group and providing me with the financial assistance and most importantly believing in me, though I was just a beginner in this field.

I would also like to express my gratitude to Prof. Sulabha K. Kulkarni for her constant support, guidance, and motivation. She has been a great mentor to me and has always encouraged me to reach heights that were beyond my expectations. I would also like to thank Dr. Angshuman Nag, Dr. Srinivas Hotha, and Dr. Pramod Pillai for their constant support, guidance, and help along the duration of this project.

I owe a profound gratitude to my senior Kavita Chandra for being a uniformly excellent advisor. I am thankful to her for helping me in every way and providing me with the much-needed guidance and support during the project.
I am also grateful to all the members of The Odom Group for their timely support, suggestions & assistance. I heartily thank all my friends for making my time memorable at IISER. I would also like to convey my regards to all of my respectable seniors especially Amey Apte, Amrit Kumar, and Prashant Bhaskar for their continuous guidance and generous support.

Above all, I would like to thank my mom, dad, and sister for their constant support and blessings.

Content

List of Figures

Abstract

Gold nanostars (NS) synthesized using Good's buffers are desirable due to their ability to produce NS with tunable branch size and number. The NS synthesized using good's buffer are bio-compatible, monodispersed, and stable over many weeks. These NS, due to their absorption in NIR and smaller size (~50 nm), have potential in imaging, bio-medicinal and surface enhanced Raman spectroscopy (SERS) based applications. This work focuses on NS synthesized using Good's buffer MOPS which has high heterogeneity and instability.

Here, we found by washing and re-dispersing the NS in DI water after synthesis, provided higher stability to the MOPS NS for over a month. Moreover, we explored the use of density gradient centrifugation for the shape separation of as-synthesized NS. Density gradient, centrifugation time and speed, and gradient steepness were optimized to separate the NS by increasing size and branch number. The sorted NS were analyzed using TEM, UV-Vis, and Dynamic light scattering. Over ~300 NS per sorted fraction were manually analyzed using ImageJ to determine the quality of separation. We found an overall decrease in the spherical NP population from 20 % to ~1% whereas an increase in NS population with high branch number from ~1% to 67% over the fractions. We also observed an increase in the average NS size and branch length from 18nm to 34nm over fractions.

Introduction

1.1 Gold

Gold is a transition metal (d- block) which is placed in group 11 of the periodic table. It is a noble metal, and highly stable in the bulk form. Gold is the second densest metal and is denoted by the symbol Au.

Atomic Number	79
Electronic Configuration	[Xe] $4f^{14}5d^{10}6s^{1}$
Atomic Mass	196.96g/mol
Density (rt)	19.30g/cm^{3}
Melting/ Boiling Point	1337.18 K/ 3243 K
Lattice Constant	0.408 nm at 300 K
Crystal Structure	Face centered cubic (fcc)

1.2 Importance of Gold Nanostructures

Gold shows characteristic properties at the nanometer range (100 nm or less) which are different from its bulk form. When $HAuCl_4$ (Au salt) is reduced using a reducing agent, it results in Au seeds formation which has dimensions in the nanometer range. When these gold seeds are dispersed in a growth solution containing Au salt and shape-directing agent, different nanostructures can form. The applications of these as-synthesized NP depend on their size, shape and surface chemistry which dictates their optical, catalytic and electrical properties[33].

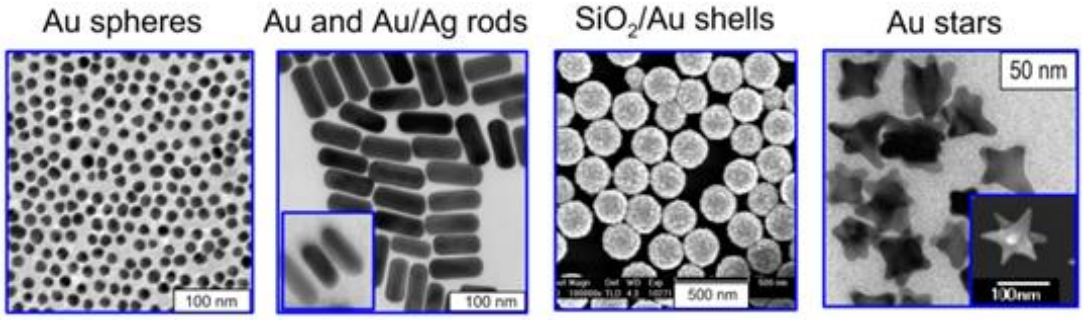

Figure 1: Different types of Au Nanoparticles (spheres, rods, shells, and Stars).[4]

1.3 Localized Surface Plasmon Resonance in Au NP

Metallic NP has plasma made of its free electrons around itself. Plasmons are the collective oscillations of free electrons, and the frequency of oscillation is termed as plasma frequency.

Au NP interaction with light is strongly dictated by their environment, size and physical dimensions. Oscillating electric field of light propagating near a colloidal NP interacts with the free electrons causing concerted oscillations of free electrons charge that is in resonance with the frequency of visible light. These resonant oscillations are known as surface plasmon resonance.

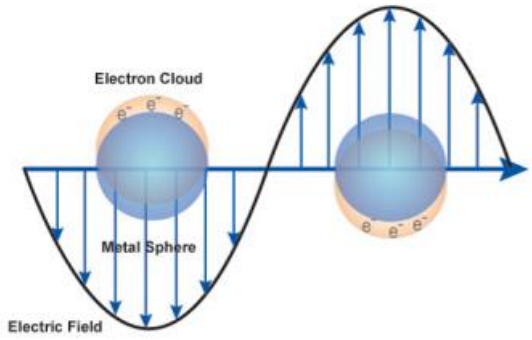

Figure 2: Schematic representation of surface plasmon polariton modes on the surface of metallic NP. [Ref: Nano & Micro systems Labs, University of Waterloo]

Localized surface plasmon resonances (LSPR) are electromagnetic modes associated with the collective oscillations of the free electrons confined to a nanoscale under resonant excitation. Anisotropic NP can concentrate the free-space optical field within subwavelength regions adjacent to their surfaces. This unique capability enables enhancement of the electric field around NP, giving rise to a variety of light-matter interactions such as Surface Enhanced Raman Spectroscopies. Anisotropic NP such as nanorods and NS poses distinct SPR modes, a longitudinal mode which is associated with electron oscillation along the length whereas the transverse mode which is associated with the electron oscillations along the transverse side of anisotropic NP.

1.4 Gold Nanoparticles Synthesis

Advancements in bottom-up approaches have resulted in the bulk synthesis of monodispersed NP with better control over their shape, size and surface chemistry. These approaches are not only inexpensive and fast compared to top-bottom approaches which require lithography but are also easily reproducible and stable. Moreover, development in bottom-up approach has now enabled the bulk production of NP with smaller sizes, not accessible using the top-down approach. Many procedures for synthesizing monodispersed NP of various sizes and shapes have been published since then. Progress in synthesis methods with better control and tunability has shifted the focus of the field on finding potential application for these materials. In last few decades, these materials have been utilized in various fields to fabricate new devices for diagnosis, sensing and to increase strength and efficiency of current materials.

Anisotropic Au NP like nanostars, nanoflowers, and nanocrystals are of particular interest because of their shape modifications such as branch number, branch length, tips and edges which can manipulate their catalytic and optical properties.[21] These NPs have LSPR peaks which are tunable throughout the visible and near-infrared (NIR) range. The characteristics features of anisotropic NP make them a good candidate for biological applications in targeted therapy[34], imaging, sensors[32] and SERS.

Out of all the morphologies, NS have drawn more attention because of their tunability in shape modification and high surface to volume ratio. Increasing interest in NS has resulted in the development of many synthesis approaches to produce NS with different symmetries using varying surfactants and reducing agents. The growth of NS requires selective capping as Au has a symmetric fcc lattice. Most of the NS synthesis procedures are two-step seed-mediated method which requires cetyltrimethylammonium bromide, polyvinylpyrrolidone, sodium citrate as shape directing agents and sodium borohydride or ascorbic acid as reducing agents. Ag^{+} is also used in many cases to tune the branch length of NS. Although these procedures have successfully able to produced NS, the two-step approach often produces a mixture of particles with different shape and size. In addition, the NS synthesized using these methods have less applicability in biomedical applications due to use of toxic chemicals like CTAB or hexadecylamine during their synthesis. Now, research

is being re-directed to produce anisotropic NP using green synthesis and non-toxic chemicals. The use of biocompatible good's buffer to synthesis NS with tunable size have curtailed the use of toxic surfactants, reducing agents and other shape directing agents.

1.5. Good's Buffer based Nanostars

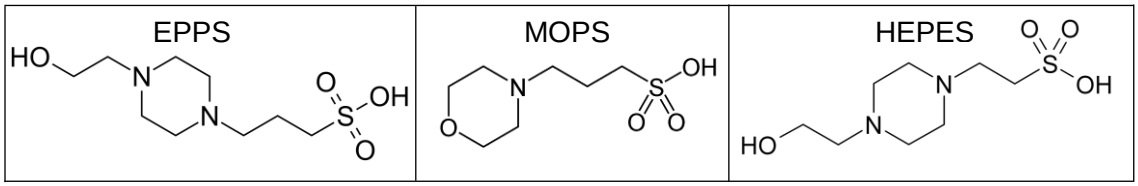

Figure 3: Molecular structure of Good's buffer EPPS, MOPS, and HEPES.

In one-pot, surfactant-less synthesis, $HAuCl_4$ is mixed with a Good's buffer which acts as both a reducing and shape-directing agent to produce NS. Good's buffers are biological buffers which are extensively used in cellular and biological studies. Three good's buffers which are well known to produce monodispersed NS are 4-(2-hydroxyethyl)-1-piperazineethanesulfonic acid (HEPES), 4-(2-hydroxyethyl)-1-piperazinepropanesufonic acid (EPPS), and 2-(N-morpholino)propane sulfonic acid (MOPS).[1] The HEPES and EPPS contains a piperazine ring and a hydroxyl group, and the MOPS contain a morpholine ring. HEPES had an ethane sulfonate group whereas MOPS and EPPS had a propane sulfonate group attached to the ring. The two tertiary amines in the piperazine ring and one in morpholine ring creates cationic free radicals which reduces the gold present in the solution, whereas the alkane sulfonic acid group in these buffer attaches to the metal surface and help in the anisotropic growth of NS.[1] These buffers can produce NS with tunable size, shape, and optical properties. The buffer concentration, pH, and Au concentration play a crucial role in directing the shape and size of the NS in this synthesis.[1] The use of Good's buffers makes these NS advantageous for biomedical application as they are biocompatible and do not require any surface modification and ligand exchange. These Good's buffer based synthesis result in highly homogeneous NS with narrower absorbance peaks in NIR range. This makes NS a potential candidate for photothermal therapies due to their better light to heat conversion efficiency. Following is the proposed mechanism of NS synthesis using Good's buffer.[5]

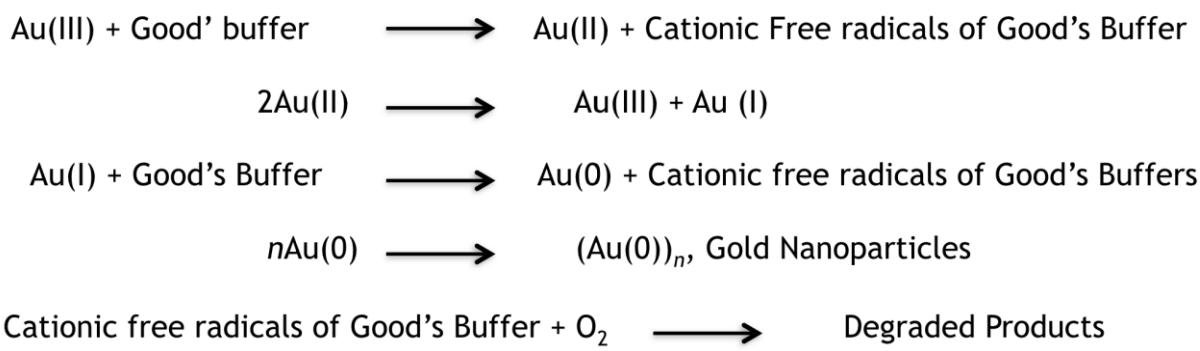

The NS produced by Good's buffers primarily differs by their branch length. The NS produced using HEPES have shortest branch length (~21nm) followed by MOPS (~36nm) and EPPS (~43nm). Also, compared to HEPES and EPPS buffer, NS produced using MOPS have the highest heterogeneity of ~40%. This is due to the absence of hydroxyl tail in the MOPS, the NS are highly unstable and turn into spherical particles over a period of 12 days.[1]

Buffer	**Heterogeneity**	**Branch length**	**Stability (over days)**
HEPES	~10%	21 $\pm$ 2 nm	> 30 Days
MOPS	~40%	36 $\pm$ 4 nm	< 12 days
EPPS	~20%	43 $\pm$ 2 nm	> 30 Days

1.6 Importance of Homogeneous nanoparticles

Monodispersed metal NPs with narrow size distribution are necessary to exploit NP's shape and size dependent properties. Generally, two strategies have been employed to obtain homogeneous NP solution: pre-synthesis and post-synthesis techniques.

1.6 .1 Pre- Synthesis Techniques

To achieve monodispersed anisotropic NP, two main factors have to be taken care of:

1) Reducibility of reductant, which controls the rate of Au reduction and helps in controlling the polydispersity of solution. When a strong reducing agent such as

$NaBH_4$ is used, the fast reduction of Au (III) to Au (0) cause secondary nucleation and thus produces heterogeneous NP. The use of a mild reducing agent such as citrate,[6] ascorbic acid,[7,8] hydroxyl amine,[9] and hydrogen peroxide[10] help in obtaining homogeneous NP by avoiding secondary nucleation.[11] The seeds formed using mild reducing agent act as a catalytic center by providing a surface to other Au atoms for reducing on and thus improves the homogeneity of the solution by allowing the controlled growth.

2) Controlling deposition of atoms on certain facets to influence the growth of NP. To achieve better control over the growth of NP and to increase the homogeneity, several approaches have been deployed such as (a) use of surfactant to promote the growth on a particular uncovered facet,[12] (b) use of additional ions in growth solution to alter the growth,[9] (c) use of different macromolecule as both reducing and shape-directing agent,[13,14,15] (d) tuning the reactivity of gold ions for preferential growth,[16] and use of Ag^+ for producing NP with longer branches by increasing facet selectivity.[19] Significant improvement has been made to control the synthesis of anisotropic NP. The growth of NP with specific size or length is now possible using epitaxial growth approaches.[18] In all of these approaches, the growth of NP is strongly directed by the kinetics and the reaction condition. The resulting synthesized NP are thermodynamically unstable and therefore transform into more thermodynamically stable structure i.e. spheres over days.[17]

1.6.2 Post-Synthesis Techniques

Most of the solution based synthesis yield polydispersed mixtures and therefore require post-synthesis separation. Separation of NP solution is the carried out to achieve mono-dispersed NP with narrow shape and size distribution. Most of the available separation techniques for NP are standard purification technique such as size exclusion chromatography,[22,23] filtration,[23,24] electrophoresis,[22,28,29] and centrifugation,[25,26] selective precipitation[27] and oxidation or etching.[3] Centrifugation-based separation is the most common and frequently used technique as it does not require any liquid –solid phase interaction. This technique separates the particle on the basis of their size and shape and further improves the resolution in presence of density gradient. Recent studies on shape and size separation of NP like Au

nanorods,[30] stars,[31] and SWCNT using density gradient centrifugation (DGC) has presented DGC's capabilities to successfully sort complex nanostructures with good resolution and has also established it as one of the most preferred technique in nanoseparation.

1.7 Density Gradient Centrifugation

DGC is a post-synthesis separation technique, in which a mixture of particles is layered over a vertical column containing viscous media with increasing density from top to bottom. DGC separates particles according to their rate of sedimentation through a viscous medium under the influence of centrifugal force. The NP move down through the density medium, and form zones containing particles of similar sizes. The viscosity of the medium amplifies the spatial separation of the particles with different hydrodynamic diameters and shapes. This technique has been extensively used for separating biological macromolecules and various NP such as rods, cubes, triangles/ prism, and nanotubes.

DGC are two types:

1) In **rate zonal centrifugation**, the sample is layered over a narrow zone on the top of a density gradient which is then centrifuged. The particles under the influence of centrifugal force begin to moves through the viscous gradient forming separate zones according to their shape, size, and sedimentation rate. This difference in sedimentation rates also prevents cross contamination of particles of different sizes and mass. The rate zonal is useful in sorting particles with same or very similar densities but of different sizes and mass, as is the case with Au NS.
2) In **isopycnic centrifugation**, the separation is solely based on the density of the particles. The density of particles which has to be separated must be between the lowest and highest density of the gradient media in the tube. Here, the size of the particle only affects the rate with which it move in the gradient. The particles would continue to separate by their buoyancy until it reaches a zone where its density is same as of the gradient media. This separation is independent of time, which means the even long duration of centrifugation won't sediment the particles at the bottom.

Density Gradient

These are viscous media primarily used to separate particles based on their density or sedimentation rate. There are two types of density gradient:

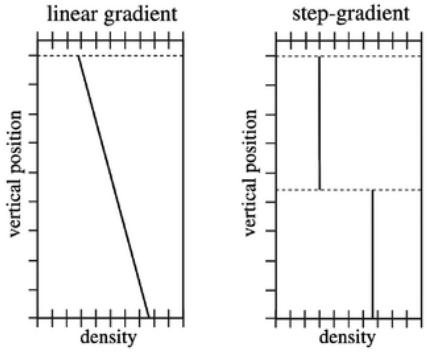

Figure 4: Schematic representation of changing density from top to bottom in linear vs. step gradient.[20]

1) Step gradient- A gradient with the successive layers of the solution with varying densities. This gradient has abrupt density steps which are useful in capturing sedimenting particles during centrifugation in different zones of two different density solutions.

2) Linear gradient- A gradient in which the density changes smoothly and progressively. This media has a continuous increasing viscosity which is important for both stabilization and nuanced separation of particles with similar features.

1.8 Theory

The use of centrifugation to sort NP is directly dependent on the shape, size, and mass of the NP, which decides its rate of sedimentation. During centrifugation, NPs undergo Brownian motion and move at different sedimentation rate depending on their mass and size. This causes sorting of NP on basis of their varying sedimentation rates. A NP moving through a viscous medium would experience three major forces which are centrifugal (F_c), buoyant (F_b) and viscous drag force (F_d).

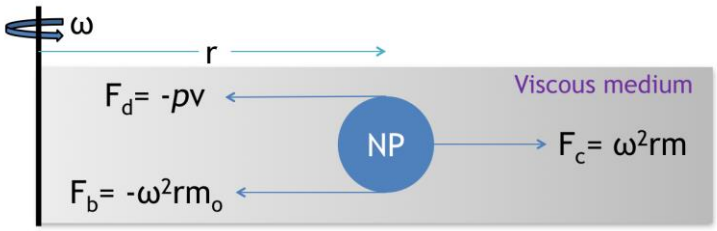

Figure 5: Schematic representation of forces acting on a NP moving through a viscous medium under centrifugal force.

Here, ω is angular velocity, r is the distance of the particle from the axis of rotation, v is the sedimentation velocity, p is drag coefficient (depends on shape and size), m is the mass of the particles whereas m_o is the mass of the fluid displaced by the particle. Under the influence of centrifugal force, the particle will move through the viscous medium until the force balances, (F_c + F_b = F_d). On equating these, we would get the Svedberg coefficient which gives the measure of sedimentation rate,[30] $v = \omega^2 r (m - m_o)/\rho$. The difference in shape and size of NP affects the rate of their sedimentation and thus sorts NP by their increasing size and mass.

Methods

2.1 Experimental Section:

2.1.1 Synthesis of MOPS Au NS:

Prepare 1M MOPS buffer stock solution and adjust its pH at 7.0 using freshly prepared 5M NaOH solution. For Au NS synthesis, Add 100 µL of 40 mM $HAuCl_4$ solution to 20 mL of 150 mM MOPS buffer (at pH 7.0) and vortex it for a minute. Keep this solution undisturbed for overnight. The as-synthesized NS were washed by centrifuging at 10,000rpm for 10 minutes and were resuspended in equal volume of water before further use.

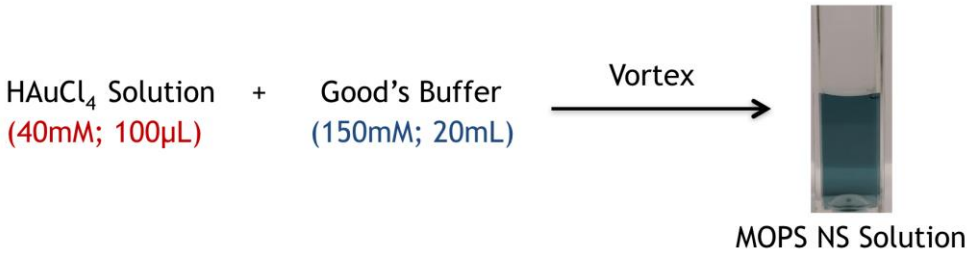

Figure 6: Scheme for synthesis of MOPS NS.

2.1.2 Preparation of Linear Density Gradient

Prepare 50 & 60% (w/v) sucrose solution in two separate containers and stir the solution until it becomes clear. Next, in a clean SETON open top centrifuging tube (25x89mm; 38.5mL) add 50% sucrose solution using a syringe till half mark. Now take a clean syringe and fill it with 60% sucrose solution and slowly start releasing the solution at the bottom of the centrifuging tube with half filled 50% sucrose solution. Again, fill the 60% sucrose solution till half mark. Now fix a rubber cap on the tube and put it in a gradient maker. To get a linear gradient, we developed a 12 step process by checking the linearity of the gradient. We collected the fractions from the gradient by going from top to bottom of the centrifuging tube containing mixture of the 50-60% sucrose solution made with the help of gradient maker. We recorded

the UV-vis spectra for each of the fractions and plotted it to check the linearity of the density gradient.

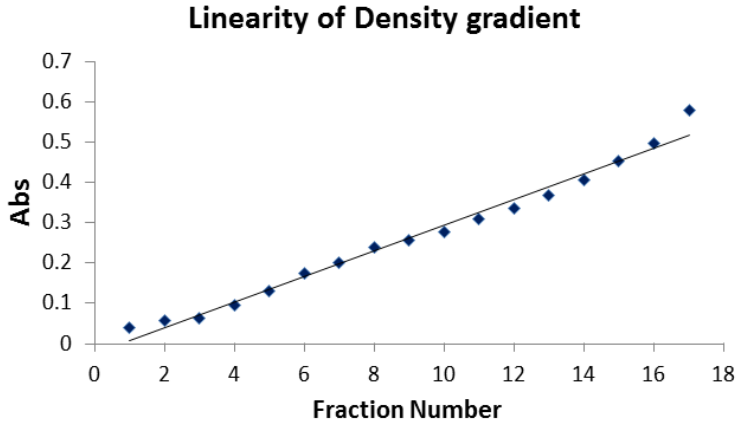

Figure 7: Trypan Blue was mixed with the 60% sucrose solution. After gradient formation, the Intensity of the ~600 nm peak was observed over fractions.

2.1.3 Layering & Centrifugation of NS solution

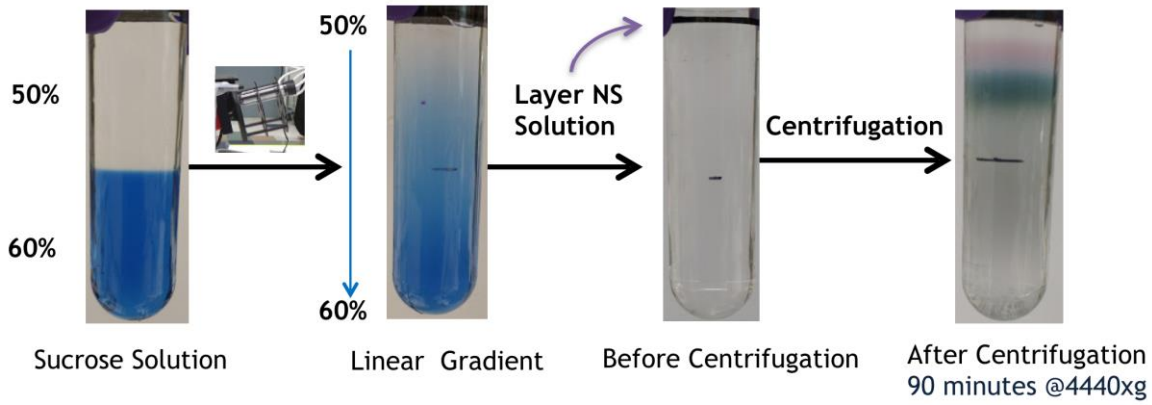

Figure 8: Gradient preparation, layering of NS solution and separation of NS using DGC. To show the linear increase in density after gradient making, Trypan blue dye has been added to the 60% sucrose solution.

20mL of Au NS solution was centrifuged (10,000 rpm, 10 min.) and concentrated to 40x times. 400 µL of concentrated NS solution was then layered over the 50-60% linear gradient using a syringe. The tube was capped and kept in a custom swinging bucket rotor (ThermoFisher centrifuge Sorvall Legend XT) without temperature

control. This gradient was then centrifuged at 4440xg for hours to get bands of sorted NS in the sucrose solution.

2.1.4 Fractionation of NS Solution

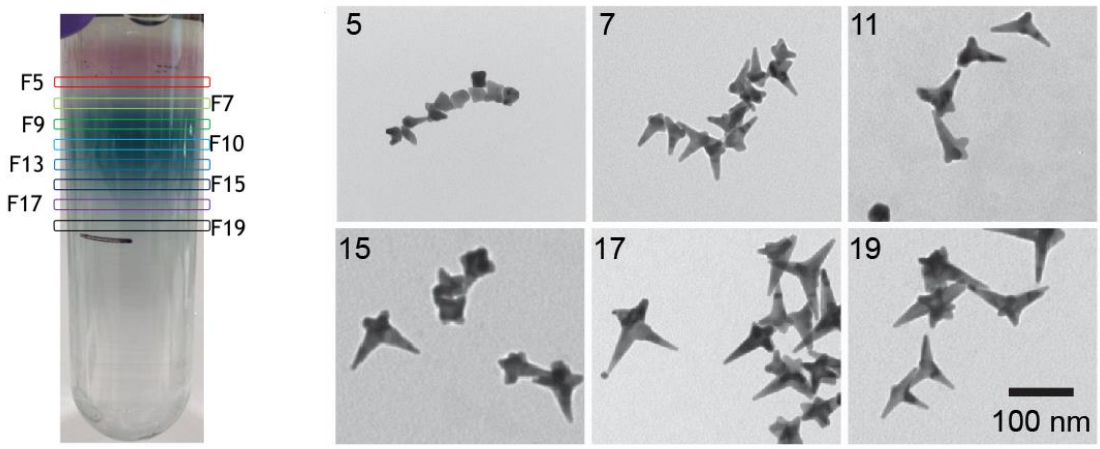

Figure 9: Picture of sorted MOPS NS and TEM images of sorted fractions from the respective regions of the tube after 90 minutes of centrifugation.

After centrifugation, Biocomp fractionator was used to collect the sorted NS from the centrifuging tube. We collected sorted NS starting from the top of the tube and by going down a fixed distance in intervals, so to have different numbers of fractions. We collected NS solution at every 2mm distance from the meniscus and repeated the step 32 times to get 32 different fractions.

2.1.5 Dialysis and TEM grid preparation

The fractionated NS were centrifuged (15,000 rpm, 20 min) and dialyzed using Thermofisher dialysis cassette (20,000 mwco*(molecular weight cut-off)). The solution was kept under slow stirring for overnight to remove the sucrose from the solution.

For TEM grid preparation, following steps were followed:

a) Cu grids were plasma treated to remove any contaminants.

b) Plasma treated Cu grids were floated over poly-L-lysine for 5 minutes. This helps in creating a positive charge over the grid.

c) 10 times concentrated NS solution (~10µL) was dropcasted over the grid and allowed to stay over it for a minute. The excess solution was carefully soaked from the grid using kemwipe.

2.1.6 Re-fractionation of sorted NS

To achieve more homogeneity, we re-fractionated the already sorted NS fractions. Due to the low concentration of NS after 1st fractionation, we combined every 2 consecutive fraction and then concentrated them 17 times before re-fractionating.

Visual observation of the initial NS separation using 50-60% gradient indicated that most of the bands were formed in the region of 50%-55% gradient and so this time instead of centrifuging the fractionated NS in 50-60% for 1.5 hrs, we centrifuged the sorted NS in 50-55% for 30-40 minutes.

After centrifugation, we collected re-fractionated NS solution at every 2mm distance from the meniscus and repeated the step 32 times to get 32 different fractions.

These fractions were then centrifuged (15,000 rpm, 20 min) and dialyzed using Thermofisher dialysis cassette (20,000 mwco). The dialysis was kept under slow stirring for overnight to remove the sucrose from the solution.

2.1.7 Characterization of NS

The NS were characterized using JEOL 1230 Transmission Electron Microscopy (TEM), Cary 5000 UV-vis NIR spectrometer, & Brookhaven's DLS particle size analyzer.

Results and Discussion

3.1 MOPS stabilization

The previous study has shown that MOPS NS are the least stable compared to HEPES and EPPS NS. The study analyzed the change in λ_1 peak using UV-Vis spectroscopy and morphology of the NS using TEM. The NS synthesized using HEPES, EPPS and MOPS were stored at 4^{o}C in growth solution over a period of 30 days to minimize the peak shift. MOPS NS over a period of 12 days showed a drastic blue shift and turned into spheres whereas the HEPES and EPPS based NS showed minor blue shift and were able to retain the morphology for over a month.

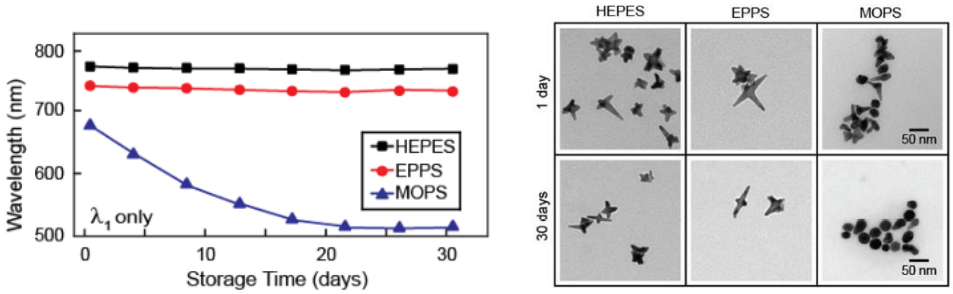

Figure 10: Shift in absorbance of λ_1 peak and over 30 days period for different good's buffer based NS when stored at 4^{o}C, supported with TEM images.[1]

The reason for the stability of HEPES and EPPS based NS is due to the presence of hydroxyl group attached to the piperazine ring which promotes the formation of self-assembled bilayer on the metal surface through hydrogen bonding and thus provides more stability to the NS structure.[1] The MOPS buffer lacks the hydroxyl group and thus we hypothesize that it fails to form any bilayer which would provide stability to the NS morphology.[1]

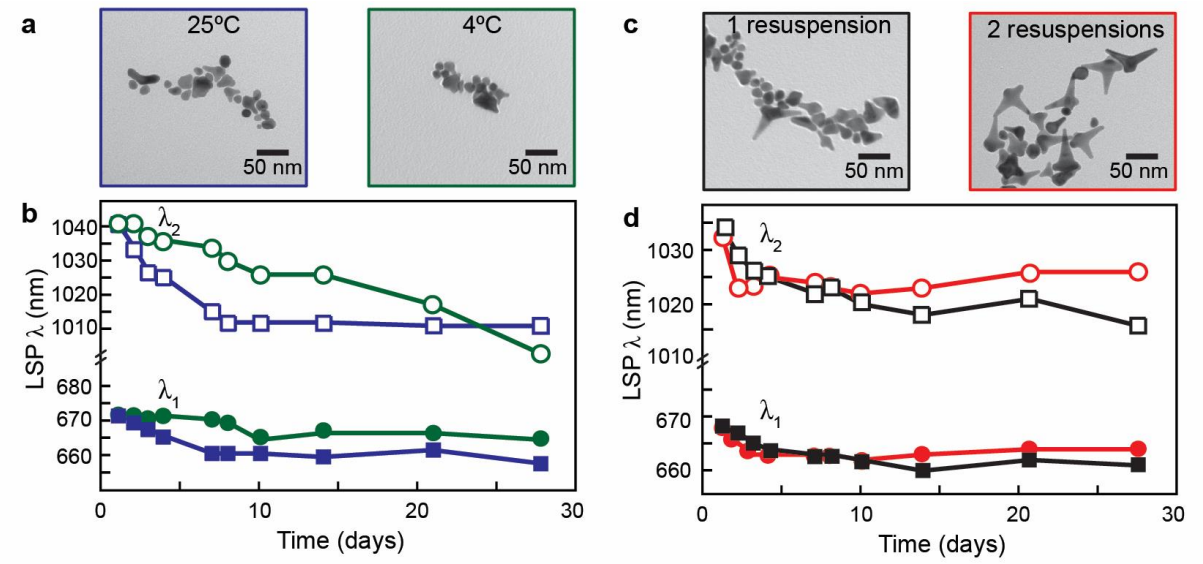

Figure 11: Stability of MOPS NS solution over days when stored at 25°C and 4°C; after 1 and 2 resuspension. a) TEM images (after 28 days of synthesis) and b) Absorbance peak shift of NS solution stored at 25°C and 4°C over days; c) TEM images (after 28 days of synthesis) and d) Absorbance peak shift of resuspended NS solution over days.

To stabilize the MOPS NS, we performed two different studies. In the first case, we observed the effect of storage temperature, and in another, we observed the effect of the number of washes and resuspension on the morphology of the NS. To study the effect of storage temperature, MOPS NS were stored at 25°C (rt) and 4°C in their growth solution (without any washing). Next, to observe the effect of the number of washing on MOPS NS degradation, NS solution were washed for different number of times and re-dispersed in Millipore water. We observed the peak shift for all the samples over 28 days and their final change in morphology using TEM.

The one time washed, and resuspended solution (1-RS) showed improvement in the shape stability than the as-synthesized solution. 1-RS retained particles with branches but showed an increase in the percentage of spherical NP. NS from 2-RS showed minimal change in shape over 30 days compared with the as-synthesized solution. Also, the 2-RS had no increase in the percentage of the spherical population. The 3-RS showed a huge loss in absorbance due to loss of most of NS which decrease the concentration of NS in the solution. In the first five days, the

resuspended NS solution showed a blue shift of 3 - 5 nm in λ_1 and λ_2 peaks whereas the as-synthesized NS solution showed a ~10 nm blue shift. After five days, 2-RS λ_1 remained constant whereas the 1-RS λ_1 blue shifted by ~3 nm. Since λ_1 corresponds to the particle core, the small shift indicated towards the presence of branched NS in resuspended NS solution even after 28 days, which was corroborated through TEM images. We also observed a fourfold decrease in the λ_1 and λ_2 peak intensity of the as-synthesized solution, whereas in the case of the resuspended NS solution a 1 to 2 fold decrease in peak intensity was observed.

The increase in the MOPS NS stability after washing and resuspension could be due to the removal of unreacted MOPS buffer from the growth solution. Morpholine based buffers, such as MOPS, are known to be unstable and degrade in solution after addition of gold. The interaction of the Au NS with the degraded or unreacted MOPS could cause colloidal instability. Therefore, the exchange of buffer solution for Millipore water through resuspension helped in stabilizing the NS.

3.2 Linear gradient vs. Step Gradient

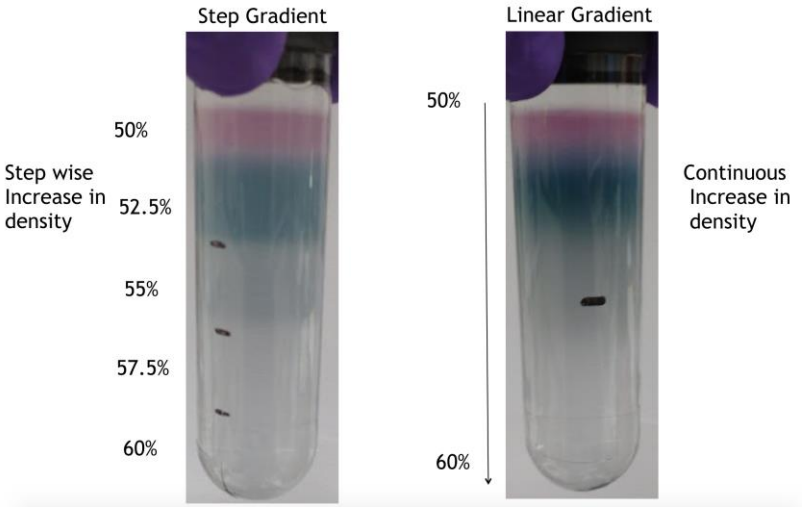

Figure 12: Sorted bands of MOPS NS in step gradient and 50-60% linear gradient.

To show the nuanced separation and importance of linear gradient over step gradient, we compared the quality of separation for MOPS NS in both step and linear sucrose gradient. Both the solutions were centrifuged at 4440xg for 90 minutes.

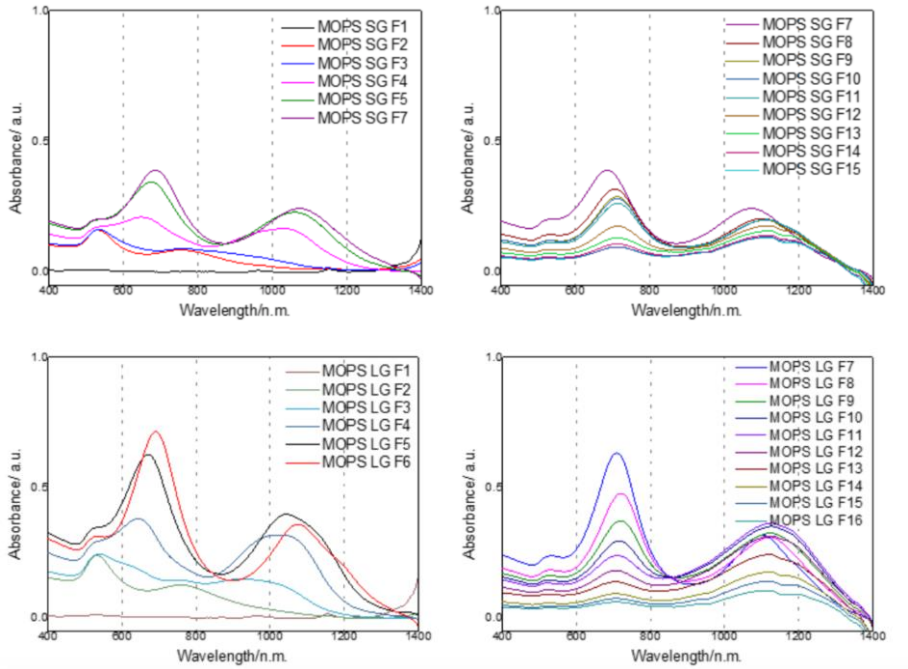

Figure 13: UV-Vis spectra of sorted fractions of NS using 50 -60% step (SG) and linear gradient (LG).

By observing the bands formation and peak shift, the quality of separation seemed to be very similar for MOPS NS. But comparing the intensity of the fractions which directly indicate the concentration of NP in the solution, we found that the sorted fraction from step gradient had lesser intensity than the sorted fraction from the linear gradient. In the case of step gradient, most of the separation was primarily happening on the basis of shape as we saw two bands with distinct colors i.e. red and blue. This indicated that NS were able to get separated from the spherical NP but were not able to separate efficiently by branch number or size. The linear gradient showed shape separation of spheres from the stars by forming two distinct bands. In addition to that linear density gradient also showed a gradual change in intensity of the bands, which indicated towards possible separation of NS by increasing size. Later, we confirmed the quality of separation by analyzing the peak shift and intensity of individual peaks using UV-Vis spectroscopy. Linear gradient not only provided better peak shift but the sorted fractions had a higher concentration of NS then the step gradient fractions.

3.3 DGC Centrifugation Time Optimization:

To overcome the heterogeneity associated with the MOPS NS and to sort them, we layered the concentrated NS solution over the 50-60% (w/v) density gradient and centrifuged it using a custom swing bucket rotor at 4440xg for 1, 1.5, 2 and 3 hours.

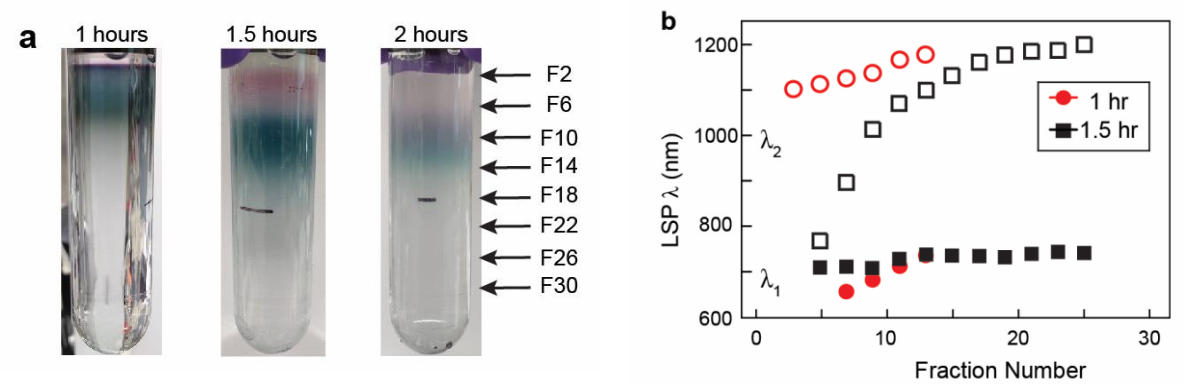

Figure 14: Sorted bands of MOPS NS. a) Band formed after 1, 1.5 and 2 hours of centrifugation. b) Shift in λ_1 and λ_2 peaks of 1 and 1.5 hour centrifuged fractions.

We focused on three parameters to evaluate the quality of separation:
a) Intensity of the sorted bands: The intensity of the band would directly relate to the population of NPs in a particular band. It would also mean less aggregation of NS.
b) Spatial distribution along the tube: A broad spatial distribution indicates a high degree of NS separation, whereas a narrow spatial distribution indicates overlapping regions of dissimilar NP.
c) Aggregation at the bottom of tube: lesser the aggregation lower is the loss of NPs, hence better separation.

In the 1 hour centrifuged tube, the Au NS solution only penetrated the 1/3rd of the gradient displaying a narrow spatial distribution and no aggregation. The 2 & 3 hours centrifuged solution led to increase in the spatial distribution but had less intense bands and high aggregation. When the centrifuged time was set at 1.5 hours, the NS solution produces a broad spatial distribution with intense bands and very low aggregation, indicating a high degree of separation.

The UV-Vis peaks of fraction from F1 to F32 were analyzed. We observed a continuous red shift in the λ_1 and λ_2 peaks of the fractions from 1 to 32, which means the fractionated NS were sorted by increasing the size and branch length.

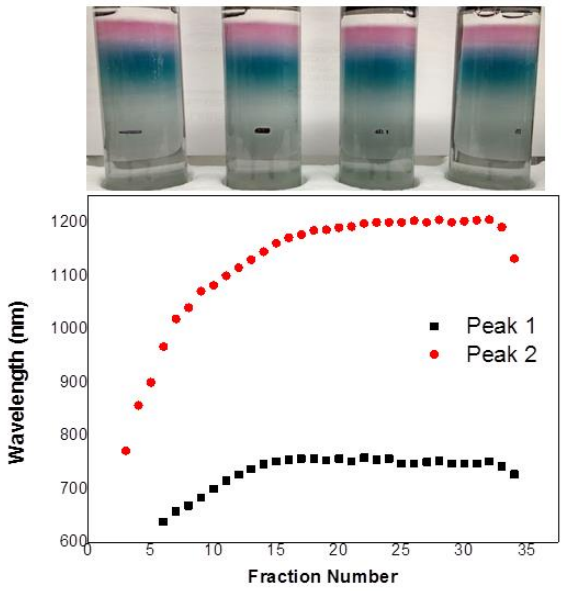

Figure 15: Reproducibility in the separation MOPS NS solution using DGC was analyzed by observing bands formed after centrifugation and by comparing the peak shift of all the sorted fractions.

We also checked the reproducibility in DGC sorting by separating multiple MOPS NS solution and analyzing the absorbance peaks of their sorted fractions w.r.t. to one another. We didn't find any inconsistency in the separation of NS solution from both visual analyses of centrifuged tubes as well as from the qualitative analysis of fractionated samples using UV-Vis spectroscopy.

The NS solution was analyzed using Brookhaven's Dynamic Light Scattering instrument for a rough estimate of NS size distribution over fractions. We found that the size of fractionated NS gradually increased over fraction from F7 to F11 and F13 to F19. The F5 and F11 showed a sudden increase in the size of NS which was not expected and could not be due to aggregates in the solution. We further analyzed these fractions using TEM for better understanding. Moreover, the DLS technique is used for symmetric and spherical NPs and so it may not give an accurate estimate for the anisotropic NP such as NS.

Fraction Number	Diameter (nm)	Poly-dispersity
F5	91.23 ± 3.01	0.324
F7	61.92 ± 1.76	0.312
F9	91.31 ± 1.11	0.273
F11	125.29 ± 1.76	0.332
F13	77.77 ± 0.50	0.310
F15	85.84 ± 2.34	0.292
F17	99.62 ± 0.11	0.305
F19	101.68 ± 0.66	0.307

3.4 NS Fractions Analysis

We centrifuged the heterogeneous MOPS NS at different time intervals to get a more homogeneous solution of NPs with similar size and shape in addition to removal of spherical particles. Out of all the 32 fractions, we chose alternate fractions for TEM analysis starting from F5 until F19 because of their peak shift and intense color bands. These fractions were dialyzed overnight to remove sucrose from the solution and later analyzed in TEM. Using ImageJ, we manually analyzed ~500 NS branches for each fraction and concluded on the quality of the separation. Further, we categorized the NS in 4 branch density population: spheres(0), low(1-2), medium(3-4) and high(5+).

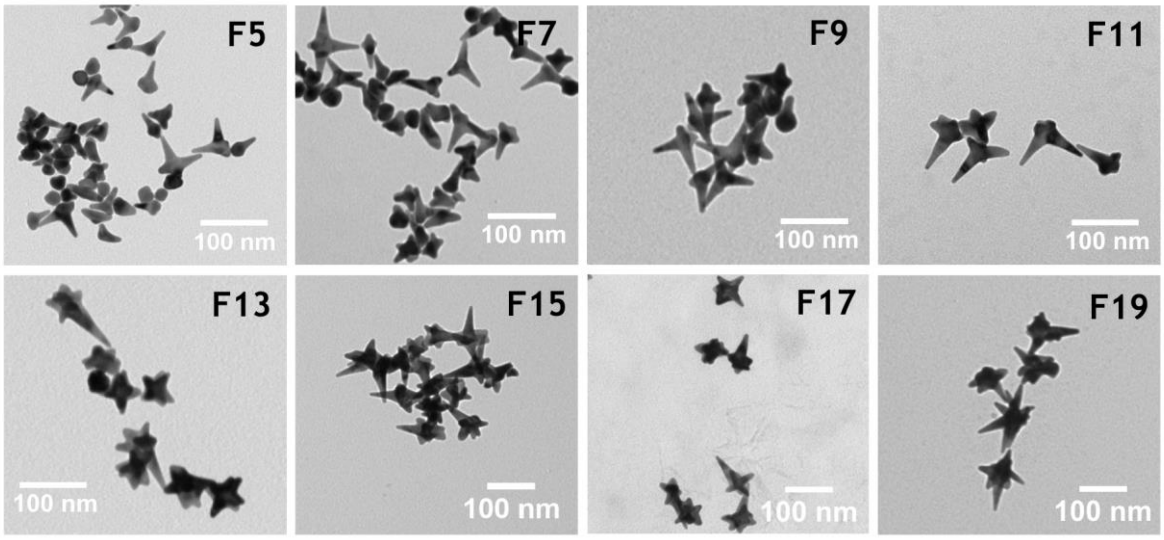

Figure 16: TEM images of sorted NS from fraction F5, F7, F9, F11, F13, F15, F17 & F19.

We observed a decrease in the sphere% from 20.12 to 0.71 over F5 to F13. This low percentage of sphere population (<1%) remained in F13 to F19 too. The low-density population% also decreased from 50 to 5 over F5 to F19. This decrease in the spherical and low branch density populations within increasing fractions created highly enriched populations of branched Au NS. The population% of high branch density NS increased from 1 to 67 from F5 to F19 and the population of medium branched NS remained constant from F7 to F15, followed by a decrease from F15 to F19. We also observed an increase in the average branch length of NS from 18 ±10 nm to 32 ±18 nm over fractions.

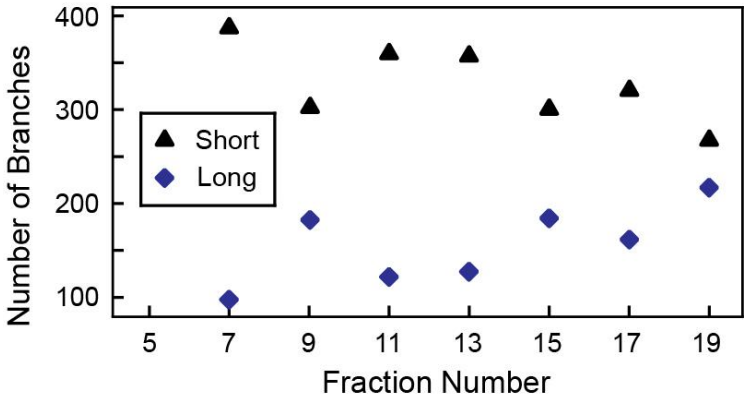

Figure 17: Plot representing distribution of number of short (<30 nm) and long (>30nm) branches over different fractions.

3.5 NS Concentration Effect on Separation

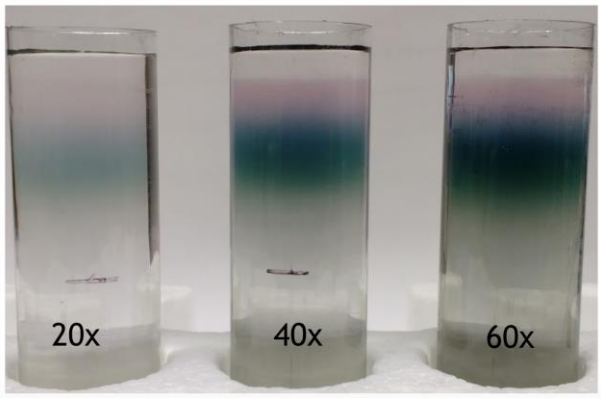

Figure 18: Sorted bands of NS solution with varying initial Au concentration (20, 40 and 60 times concentrated). The solutions were centrifuged at 4440xg for 90 minutes.

One of the important aspects in any separation technique is the initial concentration of the NP which has to be separated. And by changing the initial concentration of solute in many cases require further adjustments to be made to get the desired results. In order to check the effect of initial concentration of NS on separation, we sorted three MOPS NS solution which were 20. 40 and 60 times concentrated. 400µL of each concentrated NS solution was layered over 50-60% sucrose solution. These all were centrifuged at 4440xg for 1.5 hours and sorted into 16 fractions. The sorted fractions from each solution were analyzed using UV-Vis spectroscopy. We found all the fractions had similar peak shift trend. The only difference widely noticeable was the decrease in peak intensity which decreased as the initial NS concentration decreased. This same observation was supported from the picture of sorted bands of NS in the centrifuging tube after centrifugation. This study clarified that the quality of separation remained unaffected by the NS concentration and that this technique is scalable for effective sorting of highly concentrated NP solutions.

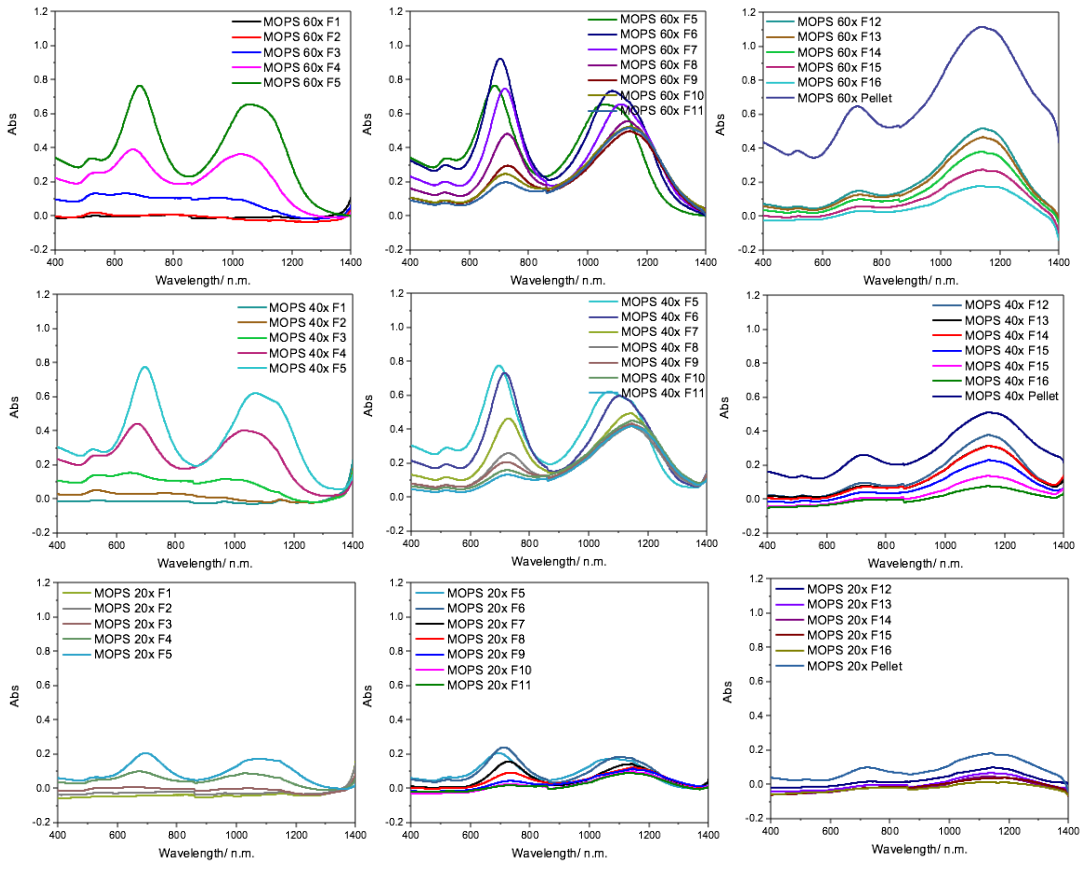

Figure 19: UV-Vis spectra of sorted NS at varying Au NS concentration (20, 40 and 60 times concentrated)

3.6 Re-fractionation

To enhance the sub-population of the already sorted fractions and to determine the extent till which the DGC could effectively sort the MOPS NS, we re-fractionated the 17 times concentrated F5, F7, F9, F11, F13, F15 and F17 fraction into 16 different fractions.

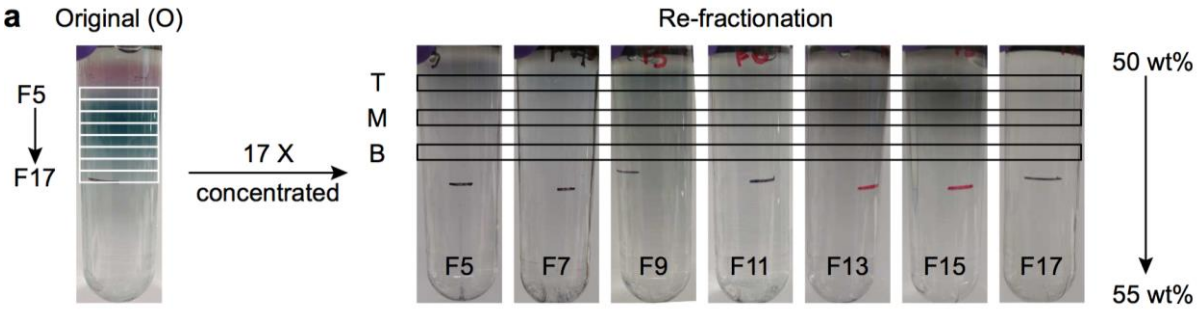

Figure 20: Picture of re-fractionated NS fractions F5, F7, F9, F11, F13, F15 and F17.

Despite concentrating the NS solution 17 times and optimizing the centrifugation time, the re-fractionated NS had least intense bands which indicated towards low concentration of re-fractions. We analyzed these fractions using UV-Vis spectroscopy and TEM. For branch density population analysis of these re-fractionated NS, we specifically chose three fractions from the top (T), middle (M) and bottom (B) of each re-fractionated NS solution. The density population of these re-fractionated NS samples was compared with their original (O) fraction.

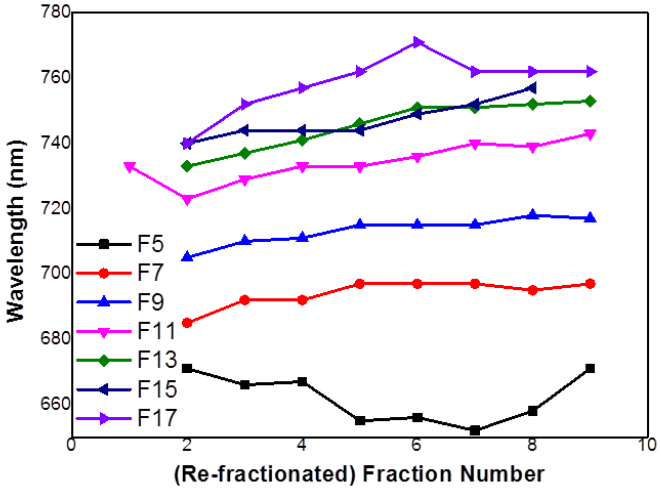

Figure 21: λ1 peak shift for re-fractionated fractions F5, F7, F9, F11, F13, F15, and 17.

We didn’t observe any clear enhancement in the population of re-fractionated fractions w.r.t to the original fraction. Although, the UV-Vis spectra for most of the fractions showed a clear red shift in λ_1 peaks except in the case of F5 and F11 where it showed an initial blue shift in λ_1 peak.

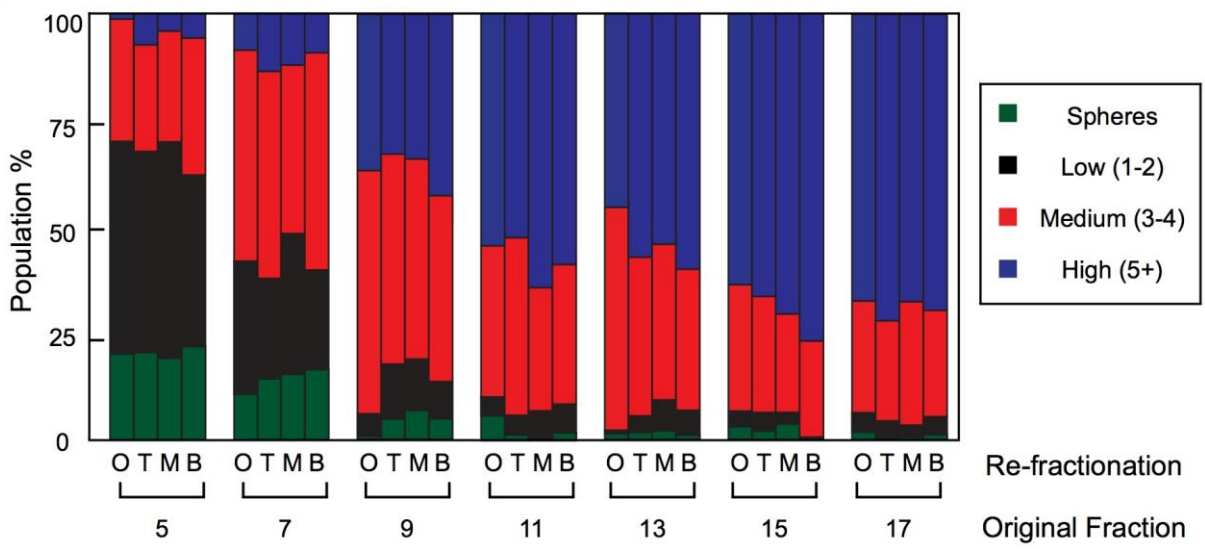

Figure 22: Branch population distribution for each of the re-fractionated sample. The Branch population from Top (T), Middle (M) and Bottom (B) of each re-fractionated sample was compared with the Original (O) sample to analyze the enhancement in the NS sub-population.

The re-fractionated fractions from the top (T), middle (M), and the bottom (B) layer of the tube didn’t show any clear distribution or increase in any particular branch density population when compared among each other. The NS population distribution for most of the fractions was similar to their original fraction. Therefore, from our study, we were also able to demonstrate limitations associated with the rate zonal centrifugation. Here, the re-fractionation of already sorted NS didn’t provide further enhancement in branch population. Thus, after initial fractionation, rate-zonal centrifugation proved to reach a saturation point after which it became inefficient in sorting similar-sized NS to further extent.

3.7 Reaction Condition Optimization:

To address the heterogeneity associated with the MOPS NS, we decided to alter the reaction conditions by varying different parameters such as the concentration and pH of the buffer, amount of Au salt and heating of the growth solution during synthesis (in a temperature controlled water bath, without any stirring). All the reactions were analyzed in UV- Vis during the synthesis at different intervals of time. After synthesis, we imaged few selected NS solution in TEM (JEOL 1230) and analyzed their branch population using ImageJ to estimate the associated homogeneity.

3.7.1 MOPS NS Reaction Optimization:

a) pH Buffer:

We synthesized NS at different pH (7 and 7.2) of the MOPS buffer by using 100µL of 40mM Au salt. It has been found that pH directly affects the stability of the NS. When the synthesis of NS is done at a pH below the pKa of the buffer, it produced stabilized NS whereas the NS aggregate when the pH is greater than the pKa.[1] The MOPS buffer has a pKa of 7.2 and so we chose to synthesize the NS at pH 7.2 & 7.

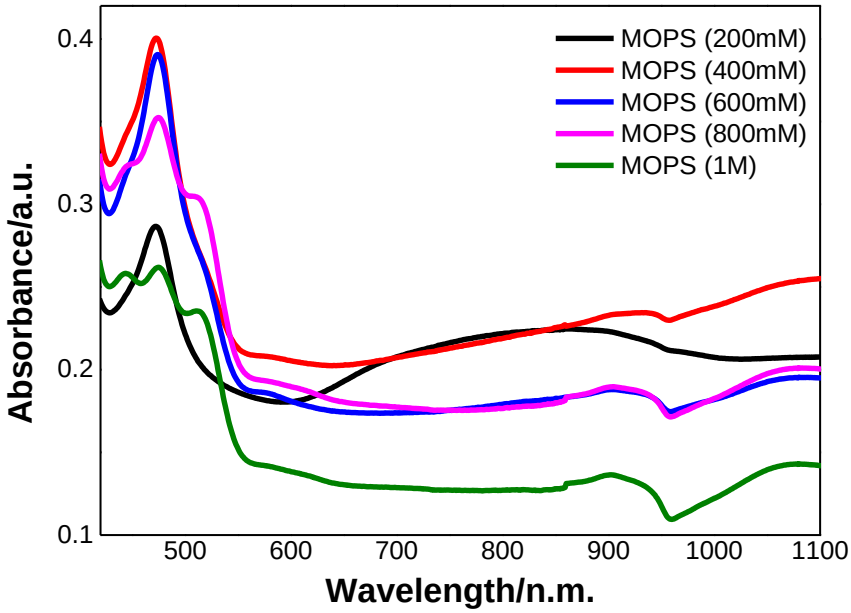

Figure 23: Absorbance spectra of MOPS NS at pH 7.2 over varying concentration.

We synthesized NP using MOPS buffer at pH 7.2 over different buffer concentrations (200mM-1M). The absorbance of all the growth solutions was observed after 30

minutes and 24 hours of reaction time to examine the peak shift over time. None of the NP solutions showed peak after 30 minutes of reaction time. After 24 hours of reaction time, all the NP solution had peak around 520 nm due to the formation of spherical nanoparticles. We also observed a broad peak ~800nm for NS synthesized at 200mM buffer which could be due to the presence of some anisotropic NP.

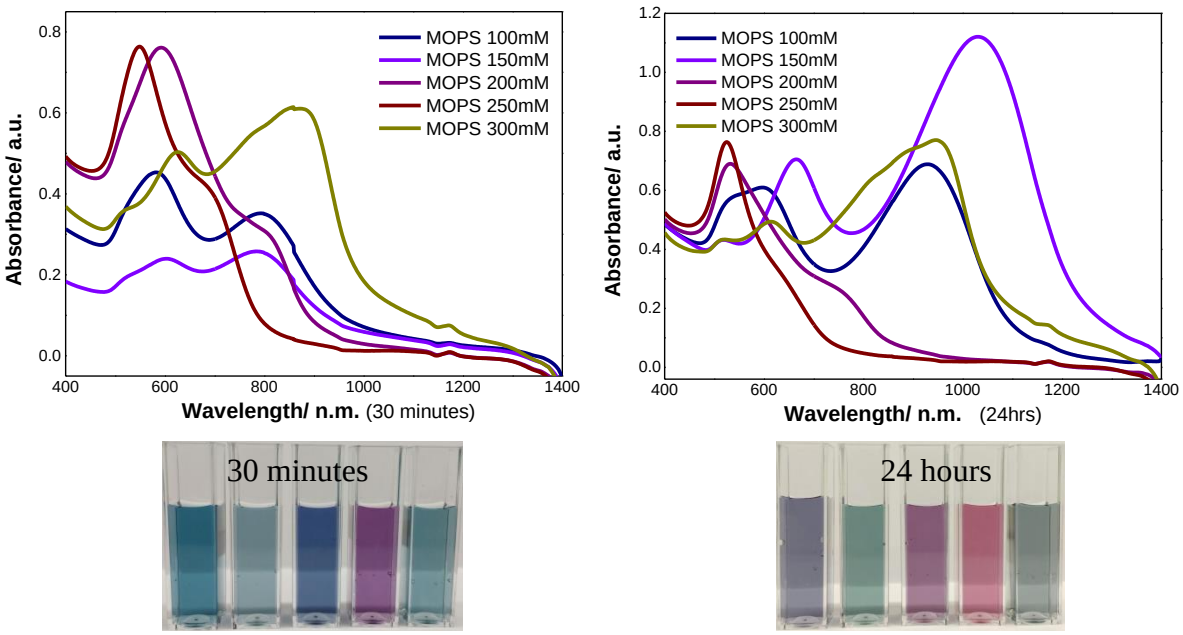

Figure 24: Absorbance spectra of varying concentrations of MOPS NS solution synthesized at pH 7, after 30 minutes and 24 hours of reaction time. The color of the solution changes overtime; L- R: 100mM, 150mM, 200mM, 250mM & 300mM.

Next, we synthesized the NP using MOPS buffer at pH 7 over the lesser concentration range (100mM - 300mM). We found that the 200mM and 250mM concentration produced spherical NP due to the presence of SPR peak at ~520nm. The 100, 150 & 300mM concentration showed two LSPR peaks after 30 minutes of reaction which later red shifted indicating towards an increase in the size or growth of branches. Out of all the concentrations, the 150mM solution had the most intense and sharp peaks in the NIR range indicating towards the longer branched NS.

b) Au Amount and Buffer Concentration Effect:

For NS synthesis, a varying amount of 40mM Au salt was added to 20 mL of MOPS buffer solution with varying concentrations. The absorbance spectra of the NS solution were recorded after 30 minutes and 24 hours of reaction time. Here, we

studied the effect of Au concentration on the reaction rate and the morphology of the NP using UV-Vis spectroscopy.

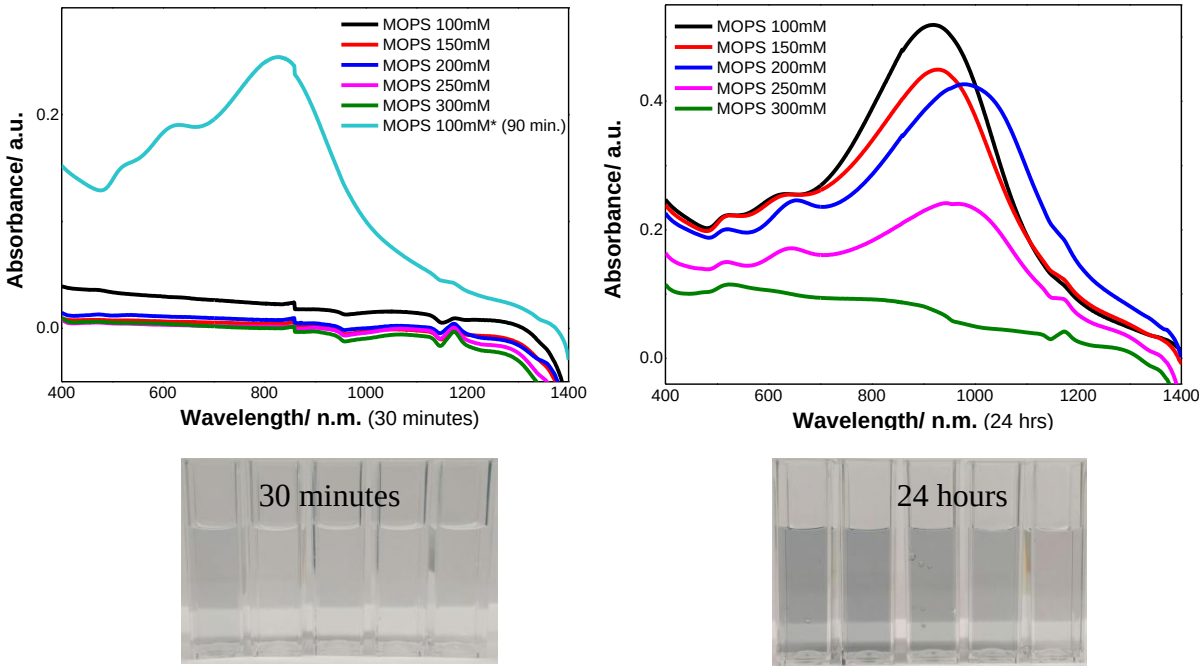

Figure 25: Absorbance spectra of varying concentrations of MOPS NS solution synthesized using **50µL of 40mM Au solution,** after 30 minutes and 24 hours of reaction time. The color of the solution changes overtime; L- R: 100mM, 150mM, 200mM, 250mM & 300mM.

A systematic study was done by varying the concentration of MOPS (at pH 7.0) and using 50µL of 40mM Au solution for synthesizing NS. No absorbance was observed after 30 minutes of reaction time. The lesser concentration of Au slowed the rate of the reaction. The MOPS solution with least concentration i.e. 100mM showed a slight change in color after 90minutes. After 24 hours, most of the solution showed three peaks at ~520nm, ~650nm and an intense and broad peak at ~900nm.

As we increased the MOPS concentration, we observed a decrease in the intensity with the slight red shift. The 300mM NS solution didn't show any absorbance and thus failed to produce NS morphology.

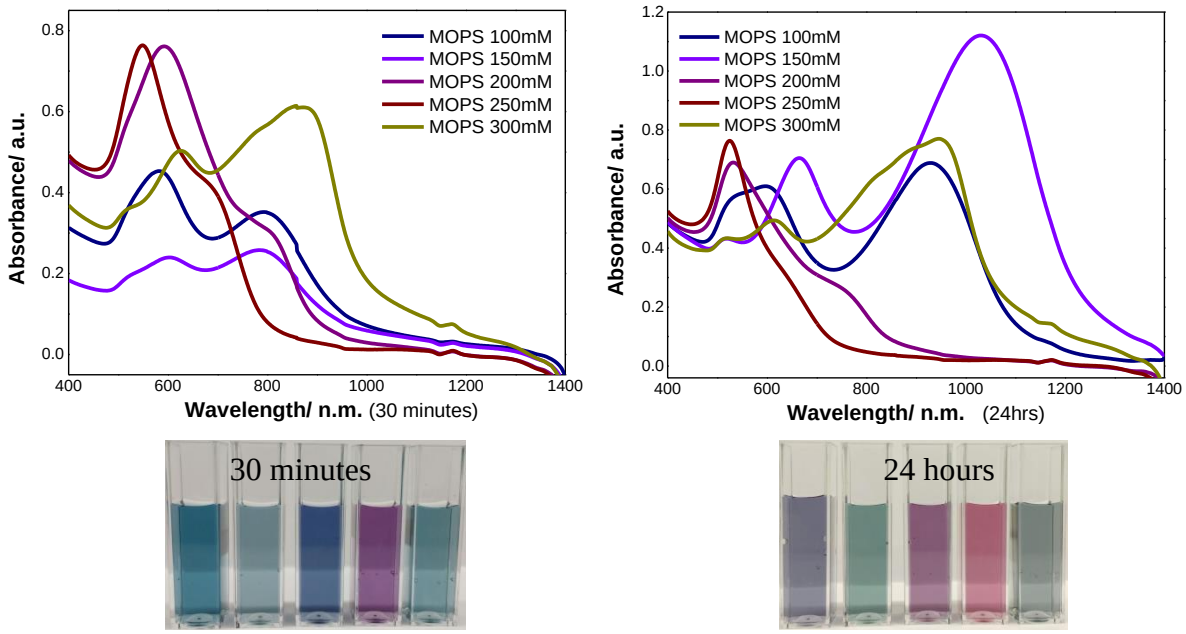

Figure 26: Absorbance spectra of varying concentrations of MOPS NS solution synthesized using **100µL of 40mM Au solution,** after 30 minutes and 24 hours of reaction time. The color of the solution changes overtime; L- R: 100mM, 150mM, 200mM, 250mM & 300mM.

Now, we synthesized the NS for varied concentration of MOPS (at pH 7) but using 100 µL of 40mM Au solution. We observed a red shift in the 100mM solution from 800nm to 950nm with an increase in intensity after 24 hrs. The 150mM solution had three peaks where the third peak being the most intense due to the longitudinal mode of SPR from the long branched NS. The 200mM and 250mM solution showed a ~520nm SPR peak indicating the formation of nanospheres in the solution.

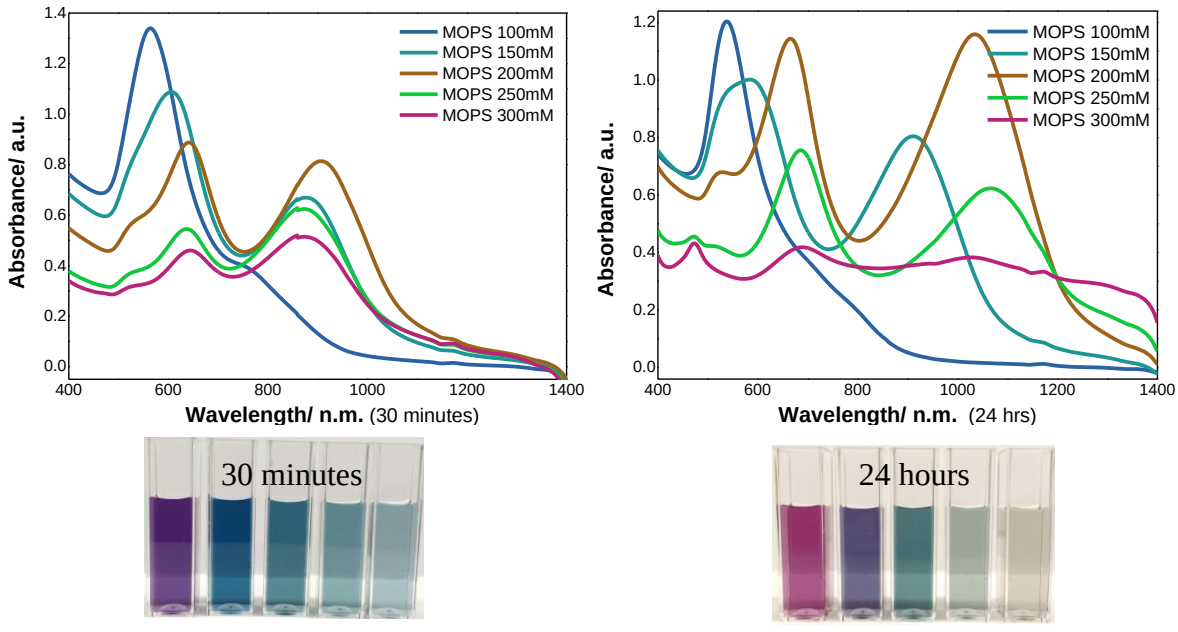

Figure 27: Absorbance spectra of varying concentrations of MOPS NS solution synthesized using **150µL of 40mM Au solution,** after 30 minutes and 24 hours of reaction time. The color of the solution changes overtime; L- R: 100mM, 150mM, 200mM, 250mM & 300mM.

At last, we synthesized the NS using 150µL of 40mM Au solution. We found that the 100mM and 150mM solution rapidly formed spherical particles and showed no significant change in the peak shift over time. The 100mM solution SPR peak was more sharp and narrower than the 150mM peak and so it seemed to have more homogeneous NP than the 150mM solution. The 200mM, 250mM and 300mM solution had three SPR peaks indicating the presence of NS. The 200mM and 250mM solution showed an increase in the intensity of the two LSPR peaks with red shift over 24 hrs time.

We found that NS solution with lower MOPS concentration had faster rate of reaction compared to higher buffer concentrations. Also, on increasing the Au solution amount in the growth solution, the reaction resulted in the formation of NP at much faster rate. We also observed that by increasing the rate of reaction (by lowering buffer concentration or by increasing Au amount) increased the chances of formation of spherical NP. Most of the NS solution synthesized using 50 and 100µL of Au solution had a slower rate of reaction which was also visible from the large change in spectra position and intensity over time. Moreover, it seemed the lower rate of reaction favored formation of anisotropic NP.

c) Buffer Concentration:

We analyzed 4 NS solution in TEM based on their absorbance peak intensity and position.

Buffer pH	**Concentration**	**Au salt (mM, µL)**	**Heterogeneity or (Sphere %)**	**Branch Population**
MOPS (pH 7)	150 mM	40mM, 100 µL	18.1%	1- 5 Branch NS
MOPS (pH 7)	100 mM	40mM, 150 µL	78.8%	1 Branch NS
MOPS (pH 7)	150 mM	40mM, 150 µL	24.2%	1- 2 Branch NS
MOPS (pH 7)	250 mM	40mM, 150 µL	17.3%	1- 4 Branch NS

d) Effect of Heating:

We heated the growth solution for 40 minutes at 40°C, 50°C, and 70°C after mixing the Au solution in the buffer. The change in absorbance spectra was observed over short intervals of time. This study was done to understand the effect of temperature on the rate of NS formation, homogeneity of the solution, and on the stability of the NS.

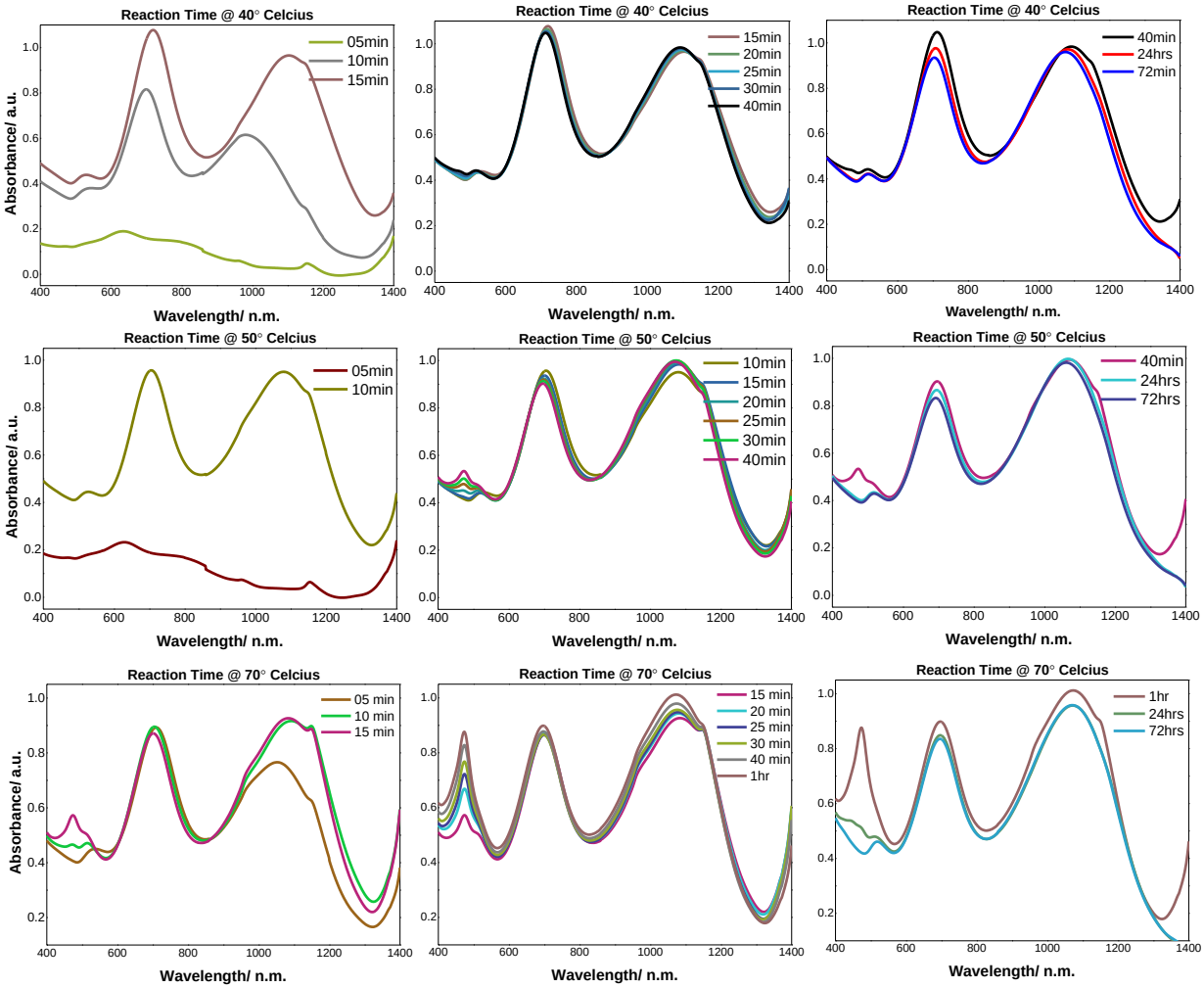

Figure 28: Absorbance spectra of MOPS NS solution at different time intervals when heated for 20 minutes at 40°C, 50°C and 70°C during the reaction.

We found that heating the growth solution during reaction increased the rate of the reaction. The Solution which was heated at 70°C reached its maximum absorbance in less than 10 minutes whereas the solution heated at 50°C and 40°C reached their maximum absorbance in ~10 and 15 minutes. The λ_1 and λ_2 peak of all the solutions showed a slight blue shift with a decrease in intensity over days. The least shift was observed for 70°C heated NS solution. During the heating time, we also observed a

new peak arising at ~480nm which diminished and disappeared as the NS solution cooled down. As the NS solution only contains Au salt and MOPS buffer, this ~480 nm peak appearance at high temperature could be related to MOPS degradation at a higher temperature.

e) Reaction Time Study of Optimized MOPS NS:

To study the reaction time of NS produced using 150mM MOPS at pH 7, we measured the absorbance of the growth solution at different interval of times and then over days.

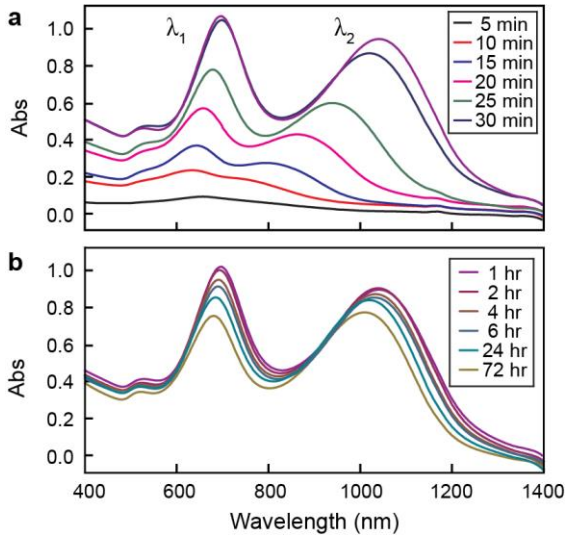

Figure 29: UV- Vis spectra of MOPS (150mM) NS growth solution over 60 minutes reaction time and for next 3 davs.

We found that the growth solution reached its peak absorbance at 60 minutes, After 60 minutes, small shifts in the absorbance occurred between 1 and 24 hours. Initially, a primary peak around ~700nm, corresponding to the core of NS rose and then a secondary peak formed ~800nm after 15 minutes of reaction time indicating growth of NS branches. Both of the primary and secondary peaks red shifted over next few minutes indicating the growth of NS and their branches. After 24 hours of the reaction, the NS solution started to show a blue shift in both the peaks with a slight decrease in intensity. This blue shift continued over next few days which implied shortening of NS branches and initiation of NS degradation.

Conclusion & Future Directions

Au NS were synthesized using Good's buffer MOPS by surfactant-less synthesis at room temperature. The synthesized NS were stabilized when washed and re-dispersed in DI water. The removal of unreacted MOPS and byproducts from the NS solution helped in stabilizing the NS morphology for over 30 days. Further, we utilized DGC for separating MOPS NS from the spherical NPs and sorted them by their increasing size and branch number. Rate-zonal centrifugation was utilized to separate the NS by shape and increasing size on the basis of their varying sedimentation rates through a 50-60% linear density gradient. The DGC based separation showed no aggregation and loss of NP during separation. We also found that varying the initial NS concentration didn't affect the quality of separation. The effect of centrifugation time and gradient type were also analyzed to optimize the sorting conditions for MOPS NS. Finally, the constraint and limitation associated with the DGC based separation were explored by re-fractionating the highly enriched population of NS to further sub-populations. Our study suggests DGC based separation is highly capable of sorting anisotropic NP with similar size and shape into enriched subpopulations. This work would help in designing strategies to sort other complex nanostructures using DGC. Moreover, these sorted NP would help in the improvement of diagnostic, imaging, SERS, and catalytic based applications.

Our future plan includes exploiting full potential of these sorted NS in enhancing diagnostic, imaging and SERS based applications. We are also interested in studying the catalytic activity of sorted NS with different branch numbers against the spherical NP with similar surface area. Further, we intend to carry out a computational study for NS separation through a dense media under centrifugal force, so to find an agreement between the theoretical and experimental results. We are also interested in developing better contrast agents for magnetic resonance imaging using gadolinium loaded NS with higher branch population. Another interesting application for sorted NS would be to study the effect of their branch number and length on the rate, orientation and preferred pathway of cellular uptake. This would provide the basis for designing next generation materials with better drug delivery capabilities.

References

1. Chandra, K.; Culver, K.S. B.; Werner, S. E.; Lee, R. C.; Odom, T.W. Chem. Mater.,2016, 28 (178), pp 6763-6769.
2. Rotz, M. W.; Culver, K. S. B.; Parigi, G.; MacRenaris, K. W.; Luchinat, C.; Odom, T. W.; Meade, T. J. ACS Nano 2015, 9, 3385−3396.
3. Kowalczyk, B.; Lagzi, I.; Grzybowski, B.A. Current Opinion in Colloid & Interface Science 2011, 16, 135-148.
4. Khlebtsov N, Bogatyrev V, Dykman L, Khlebtsov B, Staroverov S, Shirokov A, Matora L, Khanadeev V, Pylaev T, Tsyganova N, Terentyuk G. *Theranostics* 2013; 3(3):167-180. doi:10.7150/thno.5716.
5. Habib, A.; Tabata, M.; Wu, Y. G. Bull. Chem. Soc. Jpn.2005 (78), 262−269.
6. Zou, X.; Ying, E.; Dong, S. Nanotechnology 2006, 17, 4758 – 4764.
7. Jana, N. R.; Gearheart, L.; Murphy, C. J. J. Phys. Chem. B 2001 , 105 , 4065 – 4067.
8. Gou, L.; Murphy, C. J. Chem. Mater. 2005, 17, 3668 – 3672.
9. Zhao, L.; Ji, X.; Sun, X.; Li, J.; Yang, W.; Peng, X. J. Phys. Chem. C 2009, 113, 16645 – 16651.
10. Hao, E.; Bailey, R. C.; Schatz, G. C.; Hupp, J. T.; Li, S. Nano Lett. 2004, 4, 327 – 330.
11. Perrault, S. D.; Chan, W. C. W. J. Am. Chem. Soc. 2009, 13, 17042 – 17043.
12. Narayanaswamy, A.; Xu, H.; Pradhan, N.; Peng, X. Angew. Chem., Int. Ed. 2006, 45, 5361 – 5364.
13. Xie, J.; Lee, J. Y.; Wang, D. I. S. Chem. Mater. 2007, 19, 2823 – 2830.
14. Xie, J.; Zhang, Q.; Lee, J. Y.; Wang, D. I. C. ACS Nano 2008 , 2 , 2473 – 2480.
15. Kumar, P. S.; Pastoriza-Santos, I.; Rodríguez-Gonzalez, B.; García de Abajo, F. J.; Liz-Marzan, L. M. Nanotechnology 2008, 19 , 015606.
16. Jena, B. K.; Raj, C. R. Chem. Mater. 2008, 20, 3546 – 3548.
17. Wu, H.; Liu, M.; Huang, M. H. J. Phys. Chem. B 2006, 110, 19291 – 19294.
18. Chen, S.; Wang, Z. L.; Ballato, J.; Foulger, S. H.; Carroll, D. L.J. Am. Chem. Soc.2003,125, 16186–16187.
19. Yuan, H.; Ma, W.; Chen, C.; Zhao, J.; Liu, J.; Zhu, H.;Gao, X.Chem. Mater.2007, 19, 1592–1600.

20. Kumar, A. A.; Walz, J. A.; Gonidec, M.; Mace, C. R.; Whitesides,G. M.Anal. Chem.2015, 87, 6158−6164.
21. Webb, J. A.; Erwin, W. R.; Zarick, H. F.; Aufrecht, J.; Manning, H. W.; Lang, M. J.; Pint, C. L.; Bardhan, R. J. Phys. Chem. C 2014 , 118 , 3696 – 3707.
22. J.P. Novak, C. Nickerson, S. Franzen, D.L. Feldheim, Anal. Chem. 73 (2001) 5758.
23. A. Akthakul, A.I. Hochbaum, F. Stellacci, A.M. Mayes, Adv. Mater. 17 (2005) 532.
24. S.F. Sweeney, G.H. Woehrle, J.E. Hutchison, J. Am. Chem. Soc. 128 (2006) 3190.
25. G. Chen, Y. Wang, L.H. Tan, M.X. Yang, L.S. Tan, Y. Chen, H.Y. Chen, J. Am. Chem. Soc. 131 (2009) 4218.
26. M.S. Arnold, S.I. Stupp, M.C. Hersam, Nano Lett. 5 (2005) 713.
27. K. Park, H. Koerner, R.A. Vaia, Nano Lett. 10 (2010) 1433.
28. J.P.A. Isabelle Arnaud, C. Roussel, H.H. Girault, Chem. Commun. (2005) 787.
29. M. Hanauer, S. Pierrat, I. Zins, A. Lotz, C. Sonnichsen, Nano Lett. 7 (2007) 2881.
30. B. Xiong, J. Cheng, Y. X. Qiao, R. Zhou, Y. He, E. S. Yeung, J. Chromatogr. A 2011, 1218, 3823.
31. Culver, K.S.B.; Shin, Y.J.; Rotz, M. W.; Meade, T. J.; Hersam, M.C.; Odom, T. W. J. Phys. Chem. C, 2016, 120 (38), pp 22103–22109.
32. Kumar, V.; Patil, V.; Apte, A.; Harale, N.; Patil, P.; Kulkarni, S. Langmuir 2015 , 31 , 13247 – 13256.
33. Kulkarni, S. K. Nanotechnology: Principles and Practices, 3rd ed.; Springer International, 2015.
34. D. H. M. Dam, K. S. Culver, P. N. Sisco and T. W. Odom, Ther. Delivery, 2012, 3, 1263–1267.